

Electronic phenomena in reduced dimensionality systems (Scientific session of the Physical Sciences Division of the Russian Academy of Sciences, 30 October 2013)

DOI: 10.3367/UFNe.0184.201407h.0783

A scientific session of the Physical Sciences Division of the Russian Academy of Sciences (RAS), entitled “Electronic phenomena in reduced dimensionality systems”, was held on 30 October 2013 at the conference hall of the Lebedev Physical Institute, RAS.

The agenda posted on the website of the Physical Sciences Division, RAS, www.gpad.ac.ru, included the following reports:

(1) **Pudalov V M, Kuntsevich A Yu** (Lebedev Physical Institute, RAS, Moscow), **Reznikov M** (Technion, Haifa, Israel), **Morgun L A** (Lebedev Physical Institute, RAS, Moscow) “Two-phase state spontaneous emergence in a two-dimensional correlated electron system”;

(2) **Tarasenko S A** (Ioffe Physical-Technical Institute, RAS, St. Petersburg) “Transport in topological insulators”;

(3) **Dolgoplov V T** (Institute of Solid State Physics, RAS, Chernogolovka, Moscow region) “Manifestation of interactions in the transport properties of low-dimensional electron systems”.

The publication of the article based on the oral report No. 3 is presented below.

PACS numbers: **71.30.+h**, **73.40.Qv**
DOI: 10.3367/UFNe.0184.201407i.0783

Manifestation of interactions in the transport properties of low-dimensional electron systems

V T Dolgoplov

1. Introduction

This report gives a review of research works performed during the last two years at the RAS Institute of Solid State Physics (Chernogolovka), which are related to the investigation of the transport properties of two-dimensional electron systems and various structures based on them. The selection of articles was limited by two conditions: first, one of the interaction types should be essential in the phenomena investigated; second, the research should not complete the series of studies, but instead must raise new questions that need further investigation.

These articles are concerned with three lines of inquiry:

(1) the investigation of a two-dimensional electron system in an InGaAs quantum well with the Rashba type spin–orbit

coupling and the study of the junction between this quantum well and a superconductor;

(2) two-dimensional electron systems of low density with strong electron–electron interaction;

(3) the study of the interaction among electrons inside the galvanically isolated one-dimensional edge channels in a quantizing magnetic field.

As one can see from the list above, the term ‘interaction’ has various meanings throughout this review.

2. Two-dimensional electron system with a Rashba type spin–orbit coupling and the junction between this system and a superconductor

This section is mainly based on articles [1, 2]. Measurements were performed with an epitaxially grown InGaAs quantum well which is schematically shown in Fig. 1a. Similar wells were studied earlier in Refs [3–5] and it was shown that electrons in these wells can have a strong spin–orbit coupling due to the Rashba effect [6].

The Rashba effect is observed in potential wells with strong asymmetry and it is originated from an additional term

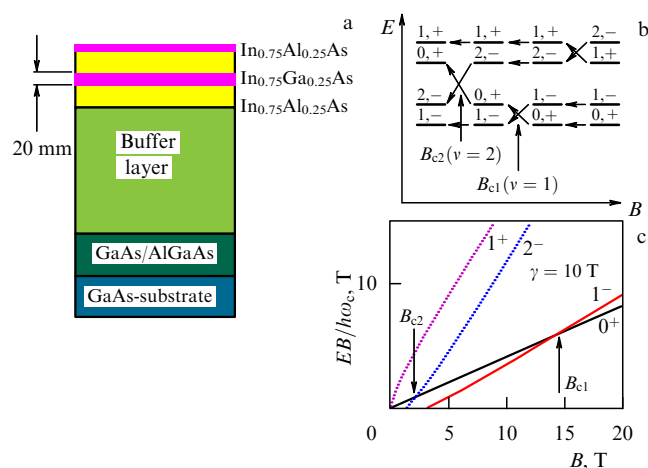


Figure 1. (a) Scheme of In_{0.75}Ga_{0.25}As quantum well growth with In_{0.75}Al_{0.25}As barriers. (b) Schematic diagram of the quantum level crossings for the Rashba type spin–orbit coupling; ν is the filling factor. (Taken from article [1].) (c) Calculated results for the positions of the lower quantum levels according to formula (2).

V T Dolgoplov Institute of Solid State Physics,
Russian Academy of Sciences, Chernogolovka, Moscow region,
Russian Federation
E-mail: dolgop@issp.ac.ru

in the electron Hamiltonian

$$\hat{H}_{so} = \alpha(\boldsymbol{\sigma} \times \mathbf{k}) \cdot \mathbf{v}. \quad (1)$$

Here, α is the interaction constant, $\boldsymbol{\sigma}$ is the vector constituted from the Pauli matrices, $\mathbf{k} = \mathbf{p}/\hbar$ is the electron wave vector, and \mathbf{v} is the unit vector perpendicular to the plane of the two-dimensional electron system. If we add this term to the regular Hamiltonian $H_0 = \hbar^2 \mathbf{k}^2 / (2m)$, the electron spectrum will split into two branches. The energy would be minimum on a circle with radius $k_{so} = m\alpha/\hbar^2$.

In a quantizing magnetic field B , the energy levels are described by the relation [6,7]

$$E_N^s = \hbar\omega_c \left\{ N + \frac{1}{2} s \left[\left(1 - |g| \frac{m}{2m_0} \right)^2 + \frac{\gamma}{B} N \right]^{1/2} \right\}, \quad (2)$$

where ω_c is the cyclotron frequency, $s = \pm 1$ for $N = 1, 2, \dots$ and $s = 1$ for $N = 0$, the effective mass $m/m_0 = 0.035$, m_0 is the free-electron mass, γ describes the spin–orbit interaction, g is the Landé splitting factor, and $|g| \leq 30$.

Expression (2) leads to multiple crossings of the quantum levels, as shown schematically in Fig. 1b. By observing these crossings in a correct sequence, one can undeniably validate that Rashba splitting takes place in a specific sample. (Actually, this test is necessary for every sample, because the magnitude of the effect and its presence are determined by the degree of asymmetry of the quantum well.)

It is well known that the positions of the conductivity maxima and minima loose their coupling with the electron spectrum in a strong quantizing magnetic field, and, for example, the minimum positions satisfy the condition $n_s = mn_0$, where n_s is the electron concentration, n_0 is the Landau level capacitance, and $n = 1, 2, 3$. Nevertheless, the level crossings can be detected, because the minimum should disappear in the vicinity of the crossing point.

The electron density had to be varied when performing the corresponding measurements, so a metal gate was deposited on the sample. The electron density within a good approximation linearly depended on the DC voltage applied between the gate and the electron gas.

Figure 2 depicts the positions of the dissipative conductivity minima in the plane (B, V_g) . As one can see from the plot,

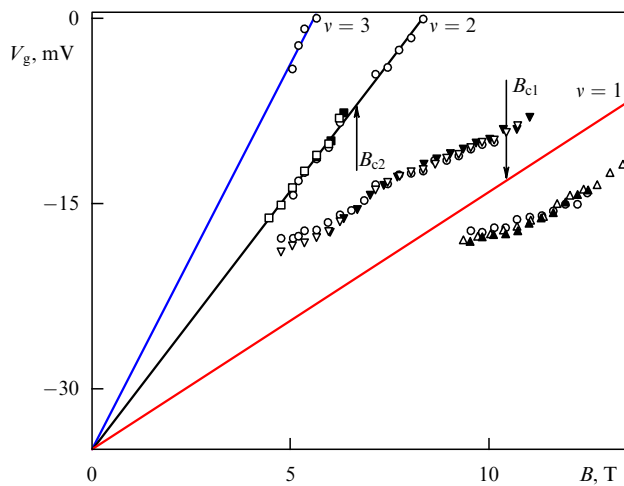


Figure 2. Dissipative conductivity minima for electrons in the study well, plotted in the plane (B, V_g) . (Taken from Ref. [1].)

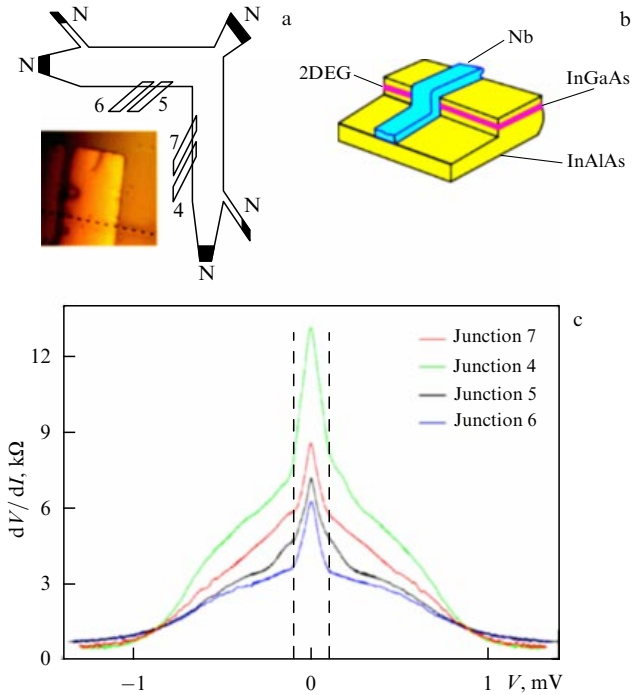


Figure 3. (a) Top view of the mesa and the junctions. N: the normal metal junctions, 4–7: the superconductor junctions. Inset: image from an electron microscope. (b) Schematic side view of the junction between a superconducting film and a two-dimensional electron gas (2DEG). (c) Experimental curves obtained for different junctions. (Taken from Ref. [2].)

the experimental points, shown with different symbols, correspond on the whole to the expected fan diagram, but the minimum disappears in the line that stands for the filling factor $\nu = 2$ in the vicinity of the magnetic field B_{c2} , and this implies the level crossing. Another feature is observed at the filling factor $\nu = 1$. Here, the minimum splits in two in the vicinity of the magnetic field B_{c1} , which also corresponds to the quantum level crossing [8]. The sequence of the crossings clearly indicates the presence of Rashba type spin–orbit splitting in the system under consideration.

However, the results obtained are not fully understood. Let us first note that the strong mismatch between the calculated results (Fig. 1c) and the magnetic field values B_{c1} and B_{c2} cannot be eliminated by varying the parameters. Most probably, the mismatch is observed because the exchange interaction was neglected in the calculations. The origin of different behaviors of the dissipative conductivity minima in the vicinity of the quantum level crossings also remains unknown. But other electron systems had this problem as well (see, e.g., paper [8]).

Samples with mesa, shown in Fig. 3a, were fabricated to study the properties of the junction between the superconductor and the electron system in the InGaAs quantum well. Neither normal metal (NiAu) nor superconductor (Nb) contacts were fired, but were thermally sputtered onto a deeply etched mesa in the way shown in Fig. 3a, b. Altogether there were five junctions with the normal metal, and four junctions with the superconductor. The junction resistance was measured at alternating current (AC) of low frequency and amplitude (in the linear regime) with the DC voltage applied to the junction (Fig. 3c).

Current–voltage (I – V) characteristics were linear in the case of a normal metal junction or in the case of a niobium

junction in a magnetic field suppressing the superconductivity. In a zero magnetic field, all experimental curves obtained for each of four niobium junctions had similar shapes (Fig. 3c). The resistance increased in the niobium superconducting gap, which is typical for Andreev reflection of electrons in the presence of tunnel resistance at the boundary normal metal–superconductor [9]. Moreover, a strong maximum of resistance was observed at low junction voltages, and it is possibly related to spin–orbit interaction. There are two facts that confirm the last statement: first, the maximum existed only at temperatures $30 \text{ mK} < T < 1 \text{ K}$, completely disappearing at higher temperatures, although the peculiarity related to the Andreev reflection remained almost unchanged. Second, the maximum was also suppressed in the magnetic field $B \approx 2 \text{ T}$ parallel to the interface, while the superconductivity was not destroyed and the Andreev reflection still took place.

At the same time, we cannot conclusively prove the fact that the spin–orbit coupling is responsible for the emergence of the maximum. Although the theory actually predicts an increase in the junction resistance under conditions similar to the experimental ones [10], but the theory has only one energy scale, namely the superconducting gap, so the narrower maximum cannot be explained. Moreover, curves similar to the one shown in Fig. 3c (zero bias anomaly, ZBA) had already been observed for some junctions between the superconductor and normal metal [11, 12]. In these articles, the anomaly is related to Coulomb blockade, which is unlikely to be the case for the effect considered. The more so that in the last experiments with InGaAs quantum wells, where NbN was used as a superconductor, there was no barrier between the two-dimensional electron system and the superconductor, but the effect was still observed.

3. Two-dimensional electron systems of low density

Two-dimensional electron systems of low density are known to have strong electron–electron coupling in the sense that the Coulomb interaction energy E_C for the characteristic distance between the electrons is significantly larger than the Fermi energy E_F (see the inset to the lower part in Fig. 4). The most convenient systems for research are the ones with a large effective mass in the plane and with the static permittivity as low as possible, all other parameters being equal. One such system is the silicon field-effect transistor.

The effect of the significant (several-fold) increase in the electron effective mass, as the electron density is reduced, was observed exactly in the two-dimensional electron gas in silicon field-effect structures [13, 14]. The electron mass enhancement was demonstrated through several experimental realizations. As an example, the results of one of the experiments are shown in the upper inset to Fig. 4 [15].

The electron spectrum in silicon field-effect structures has a two- or multiple-valley shape (it depends on the crystallographic orientation of the interface). The presence of several valleys additionally lowers the Fermi energy. Up to now, there has been no demonstration of any significant increase in the charge carrier effective mass for the lowest achievable electron densities in single-valley systems.

The question raised in article [16] can be summarized as follows: Can one detect traces of the expected increase in the effective mass in a single-valley electron system at densities that are significantly higher than the critical density n_c , at which the mass goes to infinity? The answer to this question is

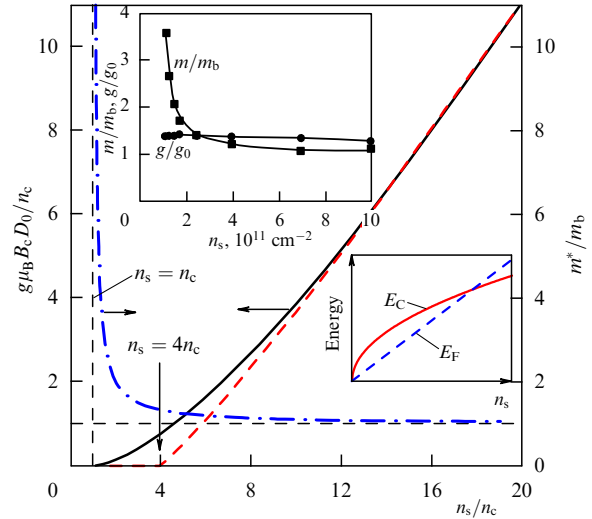


Figure 4. Electron effective mass in the one-valley two-dimensional electron system versus the electron concentration (dashed-dotted line), and the full spin-polarization field dependence as the magnetic field is increasing (solid line) and decreasing (dashed line). The upper inset shows the experimental dependences of the effective mass and the Landé factor for the silicon field-effect structure (100). (From the results in article [15].) The lower inset qualitatively demonstrates the relation between the Fermi energy of the two-dimensional electrons (dashed line) and the characteristic energy of the Coulomb interaction (solid line). (μ_B is the Bohr magneton, D_0 is the density of states of the fully spin-polarized noninteracting gas, m^* is the calculated value of the effective mass, m_b is the band value of the effective mass, and g_0 is the free-electron Landé factor.)

given by adapting the theoretical model proposed in Ref. [17] to the problem under consideration.

It is anticipated that the ground state of the electron system at low densities can be described as an electron crystal with a large number of mobile imperfections that carry the charge [18]. A real two-dimensional electron system is replaced by a grid of lattice nodes, and each of them contains either no electrons, or one electron, or two electrons with opposite spin directions. A class of trial many-electron wave functions was constructed for this model in Ref. [17], and the mean value of the Hamiltonian was obtained in Ref. [16] by utilizing an arbitrary wave function from the offered class in a parallel magnetic field with an arbitrary degree of spin polarization. As a result, the problem was reduced to the choice of an optimal trial wave function and optimal spin polarization for a fixed value of the magnetic field.

The calculated results are given in Fig. 4. First of all, let us note the result that we know already, shown on the plot with a dashed-dotted line — the effective mass goes to infinity in the zero magnetic field. But we are more interested in the behavior of the full spin-polarization field. For the case of an increasing magnetic field, it is shown by the solid line, and for the decreasing magnetic field with a dashed line. As one can see from Fig. 4, the hysteresis in the full spin-polarization field is the precursor of the effective mass divergence, and the loop can be observed for concentrations which are several orders of magnitude larger than n_c . Unfortunately, there are no corresponding experimental results yet.

Another line of research in the field of two-dimensional electron systems of low density is the measurement of the thermal electromotive force (thermal EMF) for the lowest achievable electron concentrations [19]. Silicon field effect transistors with the Hall-bar structure (see inset to Fig. 5)

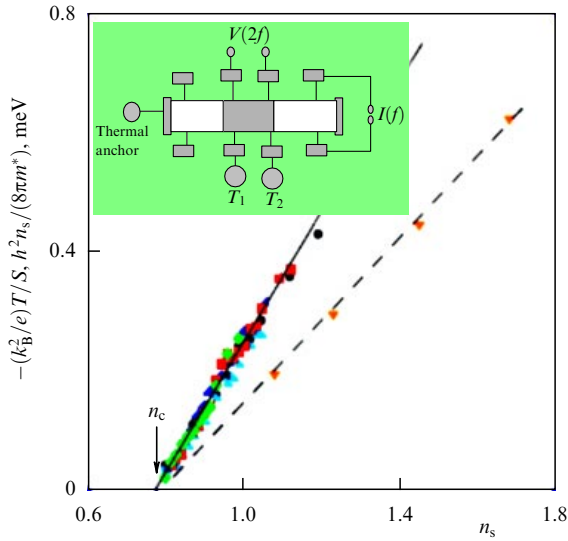


Figure 5. T/S versus n_s (solid line). The results were obtained from the measurements (shown with different symbols) for the temperatures 800, 700, 600, 400, and 300 mK. The dependence $n_s/m^*(n_s)$ (dashed line) is obtained from independent measurements with the same sample [15]. Inset: sample for thermal EMF measurements and the wiring diagram. The central part used in the measurements, where the electron concentration reached minimum values, is marked with the dark rectangle.

were tapped to perform the measurements. The region with the gate-controlling electron density was situated in the center of the bar (marked with dark color). One of the source–drain contacts was in good thermal contact with the helium bath and played the role of the thermal anchor. The electron system was heated by running a low-frequency current through the pair of potential contacts in that part of the sample where the electron concentration was relatively large ($\geq 3 \times 10^{11} \text{ cm}^{-2}$). Another pair of potential contacts was used for thermal EMF measurements (at doubled frequency of the heating current), and two more potential contacts allowed measuring the temperature gradient. The sample was placed in a vacuum and its geometry gave the opportunity to perform multiple tests. One could change, for example, the direction of the heat flow or employ the contacts that were initially measuring the temperature gradient to measure the thermal EMF.

The idea behind the measurements was to try to obtain information about the electron effective mass for the electron densities region, where other methods do not work. It was hoped that the thermal EMF in this case would be beneficial, based on the extrapolation of our knowledge from the region of weak electron–electron interaction to the region of strong interactions. According to this knowledge, the thermal EMF is weakly sensitive to the random potential with which electrons interact. Indeed, the thermal EMF according to the calculations has the form [20]

$$S = -\alpha \frac{2\pi k_B^2 m^* T}{3e\hbar^2 n_s}, \quad (3)$$

where e is the electron charge, and the parameter α depends both on disorder and on electron–electron interaction.

The results of the measurements are demonstrated in Fig. 5, where the dependence of T/S on the electron concentration is shown for several values of the temperature. Let us first note that the experimental results are in very

good agreement with expression (3) on the assumption that $\alpha = \text{const}$ and $m/m^* = (n_s - n_c)/n_s$. The latter relation is illustrated in Fig. 5 by the dashed straight line as the function $n_s/m^*(n_s)$, obtained from the results of the independent experiment [15] with the same sample.

Earlier, it was revealed that the effective mass does not depend on the degree of spin polarization [21]; thus, a very interesting task is to perform the measurements of the thermal EMF in a magnetic field that is parallel to the plane of the two-dimensional electron gas.

4. Study of the interaction among the electrons inside the galvanically isolated one-dimensional edge channels in a quantizing magnetic field

This section is based on articles [22, 23]. The experiment was performed on single GaAs/AlGaAs heterojunctions of high quality with the electron concentration of $9.3 \times 10^{10} \text{ cm}^{-2}$ and mobility $\mu = 4 \times 10^6 \text{ cm}^2 \text{ V}^{-1} \text{ s}^{-1}$. The electron gas plane was cut into two galvanically independent parts, say ‘upper’ and ‘lower’, by applying a negative voltage to the narrow metal gate. The minimal geometrical width of the gate was less than 2500 Å. The magnetic field was directed normal to the plane of the two-dimensional electron gas, and its value satisfied the condition that the filling factor equal unity, $\nu = 1$.

The study of this structure is motivated by the following consideration: the structure described above can turn out in the quantizing magnetic field to be a promising model tool for investigations of Luttinger-liquid properties [24].

Indeed, the Luttinger model describes one-dimensional fermions with a linear dispersion relation:

$$\varepsilon = v_F \mathbf{p}, \quad (4)$$

where v_F is the Fermi velocity, and \mathbf{p} is the fermion momentum. It is assumed that fermions with the opposite signs of the Fermi velocity are distinguishable and their creation and annihilation operators (unlike the operators for real particles) are anticommutative. Finally, the fermions interact with each other, but the interaction constants for the fermions with opposite and with the same velocity directions are different.

The assumptions made by Luttinger are in good agreement with the properties of the electrons that move in oppositely directed edge channels (see, for example, Ref. [25]), which are separated by a small distance. Only the electron spectrum has a perceptible difference. Unlike the spectrum described by Eqn (4), the electron spectrum of the edge channel at an electrostatically formed boundary has a plateau at the Fermi level [26].

It is convenient that electrons moving along the lower and upper boundaries of the gate that cuts the plane can be spatially separated by a large distance, so that the electron distribution functions in each of the edge channels can be controlled before and after the region of interchannel interaction. A nearly closed quantum contact was used for the perturbation of the distribution function in one of the edge channels. To control the distribution function in the other channel, either a similar quantum contact or an electrostatically formed quantum dot was used. The process of energy transfer between the edge channels in the interaction region was studied for the nonequilibrium electron distribution formed in one of the channels with a distribution function that differed significantly from the Fermi step.

It should be noted that for the absolutely smooth boundary between the channels with no imperfections such an energy transport is actually forbidden. This conclusion can be made relying both on the consideration of weakly interacting edge channels as two independent channels with electron–hole pair creation taking place in both of them [22] and on the Luttinger-liquid model by considering the back-scattering of the elementary excitations in this liquid—plasmons [23]. The real boundary always has imperfections and its roughness is not zero, so the prohibition is naturally removed.

The energy transport between the edge channels in the interaction region was indeed experimentally revealed, and it was demonstrated that this phenomenon is caused by the exchange of plasmons.

Acknowledgments

The author is sincerely grateful to E V Devyatov, A Kononov, V S Khrapai, M G Prokudina, and A A Shashkin for the fruitful discussions and for the permission to use in the report the results they obtained. This work was supported by RAS, the Ministry of Education and Science of the Russian Federation, and RFBR.

References

1. Kononov A et al. *Phys. Rev. B* **86** 125304 (2012)
2. Kononov A et al. *JETP Lett.* **98** 421 (2013); *Pis'ma Zh. Eksp. Teor. Fiz.* **98** 477 (2013)
3. Nitta J et al. *Phys. Rev. Lett.* **78** 1335 (1997)
4. Kita T et al. *Physica B* **298** 65 (2001)
5. Desrat W et al. *Phys. Rev. B* **69** 245324 (2004)
6. Bychkov Yu A, Rashba E I *JETP Lett.* **39** 78 (1984); *Pis'ma Zh. Eksp. Teor. Fiz.* **39** 66 (1984)
7. Bychkov Yu A, Rashba E I *J. Phys. C Solid State Phys.* **17** 6039 (1984)
8. Dolgoplov V T et al. *Phys. Status Solidi B* **243** 3648 (2006)
9. Blonder G E, Tinkham M, Klapwijk T M *Phys. Rev. B* **25** 4515 (1982)
10. Yokoyama T, Tanaka Y, Inoue J *Phys. Rev. B* **74** 035318 (2006)
11. Bollinger A T, Rogachev A, Bezryadin A *Europhys. Lett.* **76** 505 (2006)
12. Bollinger A T et al. *Phys. Rev. B* **69** 180503(R) (2004)
13. Shashkin A, Kravchenko S, in *Understanding Quantum Phase Transitions* (Ed. L D Carr) (Boca Raton: CRC Press, 2010) p. 369
14. Shashkin A A et al. *Phys. Rev. B* **76** 241302(R) (2007)
15. Shashkin A A, Kravchenko S V, Dolgoplov V T, Klapwijk T M *Phys. Rev. B* **66** 073303 (2002)
16. Dolgoplov V T, Shashkin A A *JETP Lett.* **95** 570 (2012); *Pis'ma Zh. Eksp. Teor. Fiz.* **95** 648 (2012)
17. Gutzwiller M C *Phys. Rev.* **137** A1726 (1965)
18. Dolgoplov V T *JETP Lett.* **76** 377 (2002); *Pis'ma Zh. Eksp. Teor. Fiz.* **76** 437 (2002)
19. Mokashi A et al. *Phys. Rev. Lett.* **109** 096405 (2012)
20. Dolgoplov V T, Gold A *JETP Lett.* **94** 446 (2011); *Pis'ma Zh. Eksp. Teor. Fiz.* **94** 481 (2011)
21. Shashkin A A et al. *Phys. Rev. Lett.* **91** 046403 (2003)
22. Prokudina M G, Khrapai V S “Energeticheskaya relaksatsiya v zhidkosti Lattinzhera, realizovannoi v kvantovom effekte Kholla” (“The energy relaxation in the Luttinger liquid realized in the quantum Hall effect”), in *XI Rossiiskaya Konf. po Fizike Poluprovodnikov, Sankt-Peterburg, 16–20 Sentyabrya 2013. Tezisy Dokladov* (XIth Russian Conf. on Semiconductor Physics, Saint Petersburg, 16–20 September 2013. Abstracts) (St. Petersburg: Ioffe Physical-Technical Institute, RAS, 2013)
23. Prokudina M G, Khrapai V S *JETP Lett.* **95** 345 (2012); *Pis'ma Zh. Eksp. Teor. Fiz.* **95** 385 (2012)
24. Luttinger J M *J. Math. Phys.* **4** 1154 (1963)
25. Devyatov E V *Phys. Usp.* **50** 197 (2007); *Usp. Fiz. Nauk* **177** 207 (2007)
26. Chklovskii D B, Shklovskii B I, Glazman L I *Phys. Rev. B* **46** 4026 (1992)